Catalysis Letters Vol. 106, Nos. 3–4, February 2006 (© 2006)
DOI: 10.1007/s10562-005-9622-4

Chromium supported on mesocellular silica foam (MCF) for oxidative dehydrogenation of propane

Yong-Mei Liu, Wei-Liang Feng, Lu-Cun Wang, Yong Cao*, Wei-Lin Dai, He-Yong He, and Kang-Nian Fan

Department of Chemistry & Shanghai Key Laboratory of Molecular Catalysis and Innovative Materials, Fudan University, Shanghai 200433, P.R. China

Received 5 August 2005; accepted 4 November 2005

A series of chromium-containing mesocellular silica foam (MCF) catalysts have been prepared and characterized in the oxidative dehydrogenation (ODH) of propane between 350 and 600 °C. It is demonstrated that the chromium catalysts supported on MCF exhibit much higher catalytic activity in terms of propane conversion and propylene yield than literature results obtained over chromium-supported mesoporous SBA-15 or MCM-41 catalysts during the ODH of propane. Enhanced catalytic performance of the chromium-containing mesoporous MCF catalysts has been attributed to the unique three-dimensional (3D), continuous, ultralarge mesopore structure of the MCF materials, which allow a much faster internal molecular transport during the ODH of propane.

KEY WORDS: chromium; propane; oxidation dehydrogenation (ODH); three-dimensional mesopores; mesocellular silica foams (MCF).

1. Introduction

The conversion of propane to propylene is an industrially important process due to the increased demand for propylene as a major building block for the production of diverse products ranging from solvents to plastics [1]. Currently, propylene is primarily produced by catalytic dehydrogenation (DH) of propane over alumina or silica-supported chromia catalysts [2,3]. However, the propane DH reaction is a highly endothermic process requiring temperatures in excess of 873 K to obtain significant yields of propylene [4]. The thermal dehydrogenation process is energy intensive and because of the high temperatures required, catalyst coking and undesired light alkanes formation are also inherent problems [5,6]. Thus, from both technological and economical points of view, the development of new less energy-intensive processes applicable for the cost reduction production of propylene is highly desirable [7,15].

Alternatively, propylene can be obtained by thermodynamically accessible oxidative dehydrogenation (ODH) of propane in the presence of oxygen or air at much lower temperatures which does not suffer from coking [7,8]. Although catalysts composed of vanadia and molybdena supported on various oxide supports have been reported to be highly selective and active propane ODH catalysts in the literature [9–13], a number of recent reports have shown that supported chromium oxides are also moderately active and selective to the ODH of propane [14–16]. In particular, promising results have been obtained when the chromia catalysts are dispersed on siliceous mesoporous materials such as MCM-41 and SBA-15 possessing well-ordered pore structures, which were found to be quite active in the ODH of propane even at temperatures as low as 350 °C [17–19]. However, to the best of our knowledge, the yield of propylene from propane ODH in the presence of oxygen or air did not achieve above 5% up to now over all reported mesoporous Cr/MCM or Cr/SBA-15 catalysts [17–19].

Mesocellular silica foam (MCF) is a newly reported aerogel-like mesoporous material composed of large uniform spherical cells (up to 50 nm) interconnected with uniformly sized windows featuring a continuous 3D mesopore system [20,21]. Especially given its continuous three-dimensional mesopore system with ultralarge pore diameters and interconnected windows, MCF materials have the advantage over their more ordered counterparts such as MCM-41 or SBA-15 of better diffusion of reactants and products and thus overcome internal mass transfer limitations [22,23]. In the present work, for the first time, we report the results of the study of the catalytic behavior in the ODH of propane of catalysts based on chromia supported mesoporous MCF silica, in which the chromium content ranged between 0.5 and 6.0 wt%. The chemical and structural characterization of these catalysts has been carried out in order to establish a correlation between catalytic activities and properties such as the molecular nature, reducibility and dispersion of the chromium species or acidity of the catalysts.

* To whom correspondence should be addressed.
E-mail: yongcao@fudan.edu.cn.

2. Experimental

2.1. Catalyst preparation

Pure siliceous MCF was prepared according to the literature method using a Pluronic P123 triblock copolymer ($EO_{20}PO_{70}EO_{20}$, $M_{av} = 5800$, Aldrich) surfactant with 1,3,5-trimethylbenzene (TMB) as the organic swelling agent with TMB/P123 = 0.5 (w/w) [20]. Briefly, a solution of P123:TMB:1.6 M HCl:TEOS = 2:1:75:4.25 (mass ratio) was prepared, stirred for 24 h at 40 °C, and then heated at 100 °C for another 24 h [20]. The solid products were recovered by filtering off and calcined at 600 °C for 5 h to obtain a white powder of MCF. Supported chromium catalysts on MCF (*n*Cr–MCF, *n* denotes the weight content of Cr atoms in the final calcined catalysts) were prepared by impregnating the as-prepared MCF with a methanol solution of $Cr(NO_3)_3 \cdot 9H_2O$ at 60 °C, and then dried at 120 °C overnight, followed by calcination at 600 °C for 4 h. For comparison, mesoporous chromia catalysts supported on SBA-15 and MCM-41 were also prepared using the same procedure. All synthesized catalysts were pressed, followed by grinding to 60–80-mesh particles for catalytic testing.

2.2. Catalyst characterization

The chromium contents in all catalysts were measured by ICP-AES after dissolution of the samples in HF/HCl solutions. The textural parameters have been measured using the BET method by N_2 adsorption and desorption at 77 K in a Micromeritics TriStar 3000 system. Diffuse reflectance UV–Vis spectra were collected on a Varian Cary 5 spectrophotometer equipped with a "Praying Mantis" attachment from Harrick. The sample cell was equipped with a heater unit, a thermocouple, and a gas flow system for *in situ* measurements. The samples were dehydrated *in situ* in dry air at 400 °C for 30 min. Spectra were recorded upon cooling down to room temperature, flowing dry air through the sample to avoid rehydration. Temperature-programmed reduction (TPR) spectra were obtained on a homemade apparatus loaded with 50 mg of catalyst. Samples were pretreated in flowing air at 600 °C for 2 h in order to ensure complete oxidation followed by cooling to room temperature in argon. Samples were subsequently contacted with a H_2/Ar mixture (H_2/Ar molar ratio of 5/95 and a total flow of 40 $ml \cdot min^{-1}$) and heated, at a rate of 10 $°C \cdot min^{-1}$, to a final temperature of 800 °C. H_2 consumption was monitored using a TCD detector.

UV–Raman measurements were carried out on a confocal microprobe Jobin Yvon Lab Ram Infinity Raman system using the UV line at 325 nm from a Kimmon IK3201R-F He–Cd laser as the exciting source, where a laser output of 30 mW was used and the maximum incident power at the sample was approximately 6 mW. The sample was loaded in an *in situ* cell and was treated in dry air at 500 °C for 1 h for dehydration [24]. In order to characterize the acidity of the catalysts, spectra of chemisorbed pyridine were monitored on a Bruker Vector 22 spectrometer using self-supporting wafers in a heatable IR gas cell. Samples were pretreated at 450 °C for 1 h under vacuum prior to pyridine adsorption. Pyridine was adsorbed at room temperature from an argon flow containing 2 vol% pyridine. The samples were heated to 100 °C and evacuated to remove physisorbed and weakly chemisorbed pyridine. Temperature-programmed desorption of the adsorbed pyridine starting at 100 °C was studied by stepwise heating of the sample under vacuum to characterize the strength of the acid sites. Difference spectra were obtained by subtracting the background (base spectrum) of the unloaded sample.

2.3. Reaction tests

The catalytic experiments were carried out in a fixed-bed quartz tubular flow reactor (i.d. 6 mm, length 400 mm) at atmospheric pressure [11,24]. Catalyst samples (60–80-mesh) were introduced into the reactor and diluted with 300 mg quartz powder (40–60-mesh) to keep a constant volume in the catalyst bed. The flow rate and the amount of the catalyst were varied to achieve different propane conversion levels. The feed was consisted of a mixture of propane/oxygen/nitrogen with a molar ratio of 1/1/4. The feed and the product gases were analyzed on-line by a gas chromatograph (Type GC-122, Shanghai). Permanent gases (N_2, O_2, CO, CO_2) were separated using a TDX-01 column connected to a TCD detector and other reaction products were analyzed employing a Porapak Q column connected to a FID detector.

3. Results and discussion

3.1. Catalyst characterization

The specific surface area (S_{BET}) and the cumulative pore volume of the parent MCF have been measured to be 660 $m^2 \cdot g^{-1}$ and 1.54 $cm^3 \cdot g^{-1}$, respectively. The nitrogen adsorption/desorption isotherms as well as the pore size distribution (PSD) of the parent MCF unambiguously reveal the characteristic three-dimensional mesocellular structure of the MCF support. Table 1 summarizes the textural results for the different chromium loaded catalysts. It is seen that the S_{BET} of the chromium-containing MCF samples is lower than that of the unloaded supports and decreases with increasing chromium contents. This decreasing trend is also shown by the data for the cell and window sizes. The results in table 1 clearly indicates that introduction of chromium causes a continuous loss of pore volume of the MCF materials, but remains significantly higher than the pore volume of Cr-containing mesoporous materials

Table 1
Physico-chemical properties of various chromia supported MCF catalysts

Catalyst	Cr-density (CrO_x per nm^2)	S_{BET}($m^2 \cdot g^{-1}$)	V_p ($cm^3 \cdot g^{-1}$)	D_c[a](nm)	T_M[b] (°C)
MCF	–	660	1.54	22.1 (7.3)	–
0.5Cr–MCF	0.095	582	1.43	17.8 (7.4)	432
1.0Cr–MCF	0.21	553	1.36	17.7 (7.3)	428
3.0Cr–MCF	0.66	528	1.20	17.6 (6.3)	410
6.0Cr–MCF	1.42	488	1.05	17.3 (6.0)	402
1.0Cr–MCM	0.15	785	0.74	2.8	419
1.0Cr–SBA	0.19	600	0.99	6.6	424

[a] Cell diameter (D_c) and window diameter (D_w, in parenthesis) obtained from nitrogen sorption.
[b] Temperature of the maximum hydrogen consumption (T_M) based on the H_2-TPR results.

prepared by use of SBA-15 and MCM-41. It is also noticeable that the PSD for the cell and window parameters of the Cr-loaded samples is narrow, indicating that the original mesocellular structure of the support has been well preserved after chromium introduction. Thus, it can be concluded that the ultralarge mesocellular-structured MCF catalysts with a high surface area and particularly high pore volume ($>1.0\ cm^3 \cdot g^{-1}$) could be obtained at all Cr loadings in the present study.

To obtain information of the molecular nature of chromium species, diffuse reflectance spectra in the UV–Vis region of MCF-supported samples were recorded and are shown in figure 1. UV bands at ca. 250 and 350 nm assignable to Cr(VI) in tetrahedral coordination [17,18,25–29] are observed for each sample, which decrease in intensity as the chromium loading increases. Meanwhile, the bands at ca. 460 and 600 nm corresponding to octahedral Cr(III) species in Cr_2O_3 or CrO_x clusters were also identified; these bands became more intense with increasing chromium content. While the present UV–Vis spectra unambiguously reflect the coexistence of both Cr(VI) and Cr(III) species for all the Cr-containing samples, it is clear that the surface contribution of Cr(VI) species as a major surface composition in the present low Cr-loaded MCF catalysts is strongly associated with the highly dispersed nature of the chromium species. Recently, the identification of a higher surface concentration of Cr(VI) species with respect to Cr(III) species at low loadings of chromium has also been reported by Santamaría-González *et al.* for mesoporous Cr-containing MCM-41 materials [27], inferring a similar dispersion behavior of chromium over mesoporous silica supports.

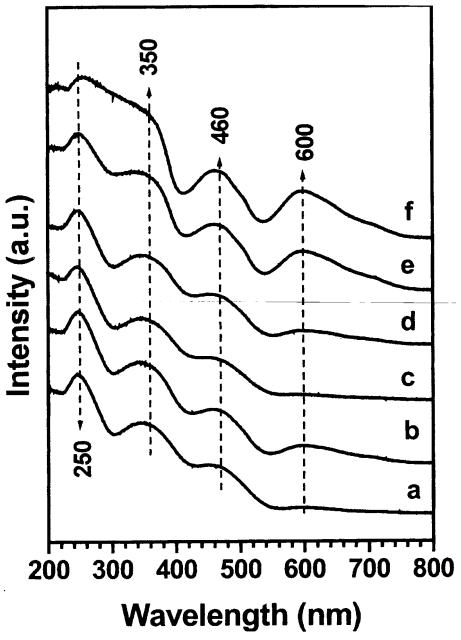

Figure 1. Diffuse reflectance UV–Vis spectra of the Cr–MCF catalysts with different chromium loading: (a) 0.5Cr–MCF; (b) 1.0Cr–MCF; (c) 1.0Cr–SBA; (d) 1.0Cr–MCM; (e) 3.0Cr–MCF; (f) 6.0Cr–MCF.

UV resonance Raman spectroscopy is a powerful technique for the study of various catalytic materials, especially for the identification of the molecular structure of low-loaded isolated transition metal atoms anchored on the surface of metal oxides [17,18,24]. It is recently established that the resonance Raman effect may provide unique opportunity to selectively enhance the intensity of the Raman signal by several orders of magnitude when the excitation laser line is close to the electronic transition absorption of the samples [17,24]. As shown in figure 1, the charge transfer of the $d\pi$–$p\pi$ transition between chromium and oxygen of chromate species occurred from 200 to 500 nm with peaks at 250 and 350 nm, thus the use of a UV laser of 325 nm as the exciting source in our measurements may cause the favorable resonance. Figure 2 shows the UV–Raman spectra of the dehydrated Cr–MCF samples along with Cr–SBA and Cr–MCM. To keep the samples dehydrated, the measurements were performed at 200 °C in flowing air after dehydration under dry air at 500 °C for 1 h. All samples exhibited an intense and sharp band located at 980 cm^{-1} assigned to the Cr–O stretching of dehydrated monochromate species (CrO_4^{2-}) [17,18]. By taking the advantage of the resonance effect of the UV line at 325 nm, Wang *et al.* have recently measured the UV Raman spectra of a series of mesoporous MCM-41 supported chromium oxides prepared by a direct

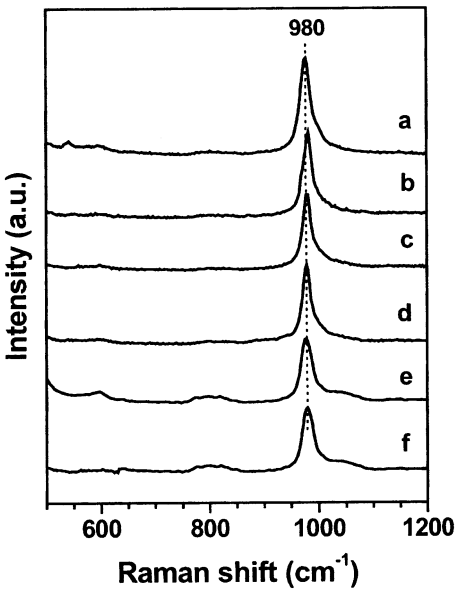

Figure 2. UV Raman spectra of the Cr–MCF catalysts with different chromium loading: (a) 0.5Cr–MCF; (b) 1.0Cr–MCF; (c) 3.0Cr–MCF; (d) 6.0Cr–MCF; (e) 1.0Cr–SBA; (f) 1.0Cr–MCM.

hydrothermal (DHT) method and a similar spectral feature at 980 cm^{-1} arising from the Cr–O stretching of dehydrated monochromate species (CrO_4^{2-}) was identified [18].

Pyridine adsorption was followed by infrared spectroscopy to identify the number and nature of acid sites in MCF-supported chromium catalysts. Figure 3 shows the FTIR spectra of the catalysts after pyridine adsorption and subsequent evacuation at 150 °C. In the spectrum of the parent MCF a band at 1445 cm^{-1} appears and is assigned to pyridine coordinatively bound to

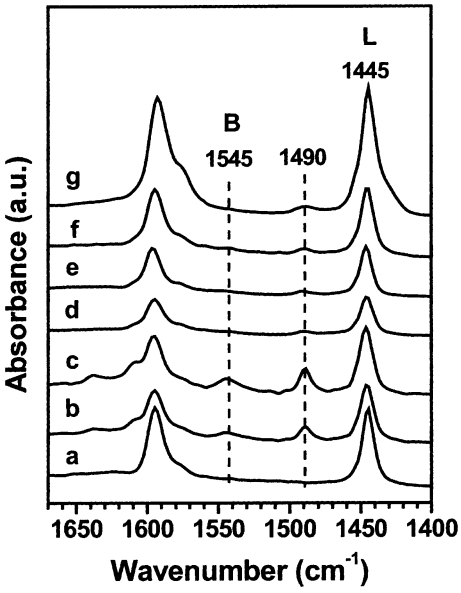

Figure 3. FTIR spectra of pyridine adsorbed on the samples: (a) MCF; (b) 1.0Cr–SBA; (c) 1.0Cr–MCM; (d) 0.5Cr–MCF; (e) 1.0Cr–MCF; (f) 3.0Cr–MCF; (g) 6.0Cr–MCF.

defect sites of a distorted silica network as weak acidic Lewis sites [29], or to hydrogen-bonded pyridine [30]. It is found that the Lewis acid sites due to parent MCF decrease substantially upon the initial anchoring of chromium on to the support surface. Nevertheless, it is seen that the number of acid sites increases with increasing chromium content for the chromium-containing catalysts, suggesting the formation of new type of Lewis acid sites on the Cr–MCF samples. Additional bands at 1490 and around 1600 cm^{-1}, associated with the presence of pyridine, are also observed in all the catalysts. However, its assignment to specific type of acid sites is not clear [31]. Thus, for the Cr–MCF catalysts studied here, only the Lewis acid sites related to chromium oxide incorporation are evidenced here, and the number of which increases with chromium loading.

It is interesting to note that an additionally weak band at ca. 1545 cm^{-1} attributed to pyridine cations formed on acidic Cr–OH groups (Brønsted sites) is registered on the spectra of the MCM-41 and SBA-15 supported chromia catalysts. Meanwhile, a close comparison of the spectra for 1.0Cr–MCF sample with those for 1.0Cr–MCM and 1.0Cr–SBA catalysts in figure 3 reveals that at the same Cr loading level the total number of both the Lewis acid sites and Brønsted acid sites is much lower on the MCF catalyst than its MCM-41 or SBA-15 counterparts. Moreover, the temperature-programmed pyridine desorption showed that pyridine adsorbed on Cr–MCF and Cr–SBA samples was completely removed by 200 °C. In contrast, complete removal of adsorbed pyridine on Cr-containing MCM-41 sample could only be achieved at temperatures well above 250 °C. Temperature-programmed pyridine desorption reveals a relatively moderate acid strength of the Lewis sites on the Cr–MCF catalysts.

The H_2-TPR profiles of Cr–MCF catalysts loaded with different amounts of chromium are comparatively shown in figure 4 and their main features are summarized in table 1. A single reduction peak with the maximum of the H_2 consumption peak (T_{max}) ranging from ca. 400 to ca. 430 °C is observed for all samples. Moreover, a progressive shift of T_{max} to lower temperatures with increasing chromium content is also observed, pointing to progressive formation of more easily reducible low polymeric chromium species [24,32]. A similar reduction peak at the same temperature range was also observed on the TPR studies of alumina and silica supported chromia samples [26]. The single reduction peak at ca. 400 °C has been attributed to the reduction process of isolated surface chromium species from high oxidation states to Cr(III), suggesting that no crystalline Cr_2O_3 is formed in alumina supported chromia [26]. It is therefore reasonable to attribute the reduction peak around ca. 400 °C to the reduction of Cr(VI) species present on the mesoporous silica supported chromia samples. It is also noticed that T_{max} of the 1.0Cr–MCF sample is slightly higher than that of

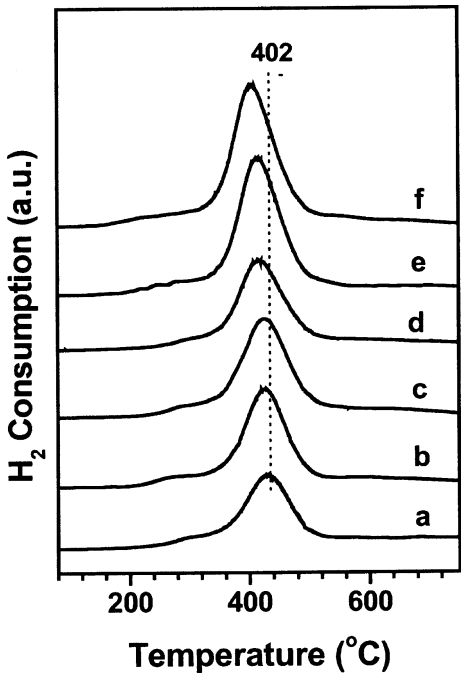

Figure 4. H_2-TPR profiles of the Cr–MCF silica catalysts: (a) 0.5Cr–MCF; (b) 1.0Cr–MCF; (c) 1.0Cr–SBA; (d) 1.0Cr–MCM; (e) 3.0Cr–MCF; (f) 6.0Cr–MCF.

1.0Cr–SBA and 1.0Cr–MCM samples, implying that the formation of highly dispersed chromium species is more favored over the surface of MCF support.

3.2. Catalytic activity

The catalytic results obtained in the ODH of propane at 550 °C over MCF-supported chromium oxide catalysts are shown in table 2. Propylene, and carbon oxides (CO and CO_2) are the main reaction products during the ODH of propane on MCF-supported chromia catalysts (table 2). It is observed that propane was poorly converted over parent MCF although the selectivity to propylene was fairly high, whereas the introduction of Cr remarkably enhanced propane conversion indicating that chromium is the active site for the ODH reaction. Propylene is formed with moderate selectivity over the MCF catalysts with higher Cr content and the propylene yield is found to be comparable with that obtained over V–Mg–O catalysts [6]. As shown in table 2, the MCF catalysts with low Cr contents would result in the formation of appreciable amount of ethylene via oxidative cracking of propane. Similar catalytic behavior has been observed over vanadia catalysts supported on mesoporous silica such as SBA-15 and MCM-41 [11,24].

The rate of propylene formation increase with the chromium loading, with a maximum value of 4.3 μmol-$C_3H_6 \cdot g^{-1} \cdot s^{-1}$ for the 1.0Cr–MCF sample, and then decreasing with increasing chromium contents. These results are expected since the monochromate species are the active centers for this reaction and the dispersion degree of chromium rapidly decreases for loadings higher than 1.0 wt%. It is also clear from table 2 that the 1.0Cr–MCF catalyst exhibited much higher propane conversion and selectivity to olefins than those of 1.0Cr–MCM and 1.0Cr–SBA samples. Note that the yields of propylene obtained over the present 1.0Cr–MCM and 1.0Cr–SBA samples are essentially comparable with that obtained over the similar Cr–MCM-41 or Cr–SBA-15 catalyst systems as reported in the recent literature [19,27]. The high selectivity to olefins on the present MCF catalysts could be related to its highly dispersed chromium species on the large surface of MCF with a large pore diameter as described above. In a comparison of three different mesoporous silica supports, it is observed that the MCF silica with a three-dimensional mesocellular foam-like structure is much superior to more structurally ordered MCM-41 and SBA-15 as a support.

The catalytic activities of the Cr–MCF catalysts were also found to be strongly dependent on the reaction temperature. To detect the possible low temperature performance of the Cr–MCF catalysts, the catalytic performance of the Cr-supported MCF catalysts with various chromium containing at temperatures between 350 and 600 °C has been investigated. Figure 5 plots the ODH of propane over the Cr–MCF catalysts as a function of reaction temperature. It is remarkable that the Cr–MCF catalysts show a high catalytic activity at reaction temperature as low as 350 °C. Note that the low temperature conversion values achieved over the present Cr–MCF systems are significantly higher than the literature data obtained over Cr-containing MCM-41 or SBA-15 materials [19,27]. In addition, it is found that the propane conversion depends strongly upon the chromium contents and for each catalyst increases rapidly with temperature. At the temperature of 600 °C, the propane conversion reaches the highest value. Moreover, the 3.0Cr–MCF catalyst is found to exhibit the maximum values of propane conversion in the whole range of temperature studied.

Figure 6 presents the variation of the selectivity to propylene with reaction temperature. It is noticeable that all the MCF loaded chromia catalysts produce propylene in the whole range of temperature studied. Previous investigations of the ODH of propane over a series of Cr-impregnated MCM-41 catalysts has shown that only the catalyst containing a Cr content of 1.5 wt% produce propylene at 350 °C, while a substantially higher reaction temperatures above 400 or 450 °C was needed for propylene formation over catalysts containing lower or higher chromium contents [27]. It is also interesting to point out that quite different behavior for propylene selectivity is observed for the different chromium loaded catalysts and the 1.0Cr–MCF catalyst exhibited the highest selectivity to propylene at higher temperature range. On the other hand, the decreased selectivity to propylene as observed for the

Table 2
Catalytic behavior of chromium supported MCF silica catalysts in the ODH of propane at 550 °C, after 360 min on-stream (W_{cat} = 50 mg, GHSV = 15,000 ml · g^{-1} · h^{-1})

Catalyst	Conversion (%)	Selectivity (%)				Rate (μmol-C_3H_6 g^{-1}·s^{-1})	TOF×10^{20}(μmol-C_3H_6 at Cr^{-1}·s^{-1})	Yield (%)
		C_3H_6	C_2H_4	CO	CO_2			
MCF	2.8	68.8	11.5	10.7	5.6	0.6	–	1.9
0.5Cr–MCF	30.8	36.6	20.2	16.2	24.9	3.5	6.0	11.3
1.0Cr–MCF	32.9	41.8	15.0	16.4	24.0	4.3	3.7	13.8
3.0Cr–MCF	36.7	31.6	11.7	22.3	32.2	3.6	1.0	11.6
6.0Cr–MCF	33.1	29.8	9.4	17.6	36.3	3.1	0.50	9.9
1.0Cr–MCM	15.2	22.9	1.5	30.8	44.2	1.1	0.95	3.5
1.0Cr–SBA	20.5	33.2	25.9	16.7	22.2	2.1	1.84	6.8

samples with chromium content higher than 3.0 wt% is possibly due to its relatively lower dispersion. As a consequence, a maximum propylene yield of 13.8% was obtained over the with 1.0Cr–MCF catalyst at 550 °C. This value was much higher than the recent literature results obtained over the conventional chromium supported MCM-41 materials [27], showing that MCF materials are promising supports for the development of high performance ODH catalysts.

Turnover frequencies (TOF), considering only the activity of Cr species, for the chromium supported samples with various chromium contents and various supports were also compared in table 2. We get a remarkable TOF value as high as 6.0 μmol-C_3H_6 at-Cr^{-1}·s^{-1} on the low loaded 0.5Cr–MCF catalyst. The isolated surface transition metal species such as vanadium or chromium moieties have been well established as the active sites in ODH of propane [17,33]. Considering the highly dispersed nature of the chromium species supported over most catalysts (except that of 6.0Cr–MCF sample) with chromium density lower than 0.7 CrO_x/nm^2 [34], it seems to be quite surprising that the Cr–MCF catalysts exhibited decreased TOF values with increasing Cr-containing. Here, the presence of small amounts of polymeric chromia species and the influence of the distance between CrO_x species on the reaction selectivity over the active sites might be considered to account for the decreased TOF values [26].

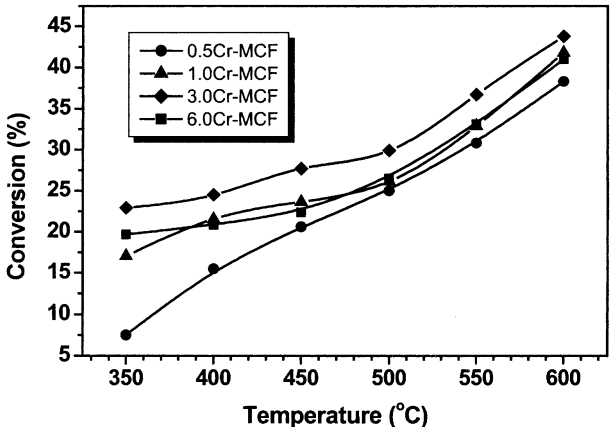

Figure 5. Conversion of propane as a function of the reaction temperature during the ODH of propane on various chromium supported MCF silica catalysts (W_{cat} = 50 mg, GHSV = 15,000 ml · g^{-1} · h^{-1}).

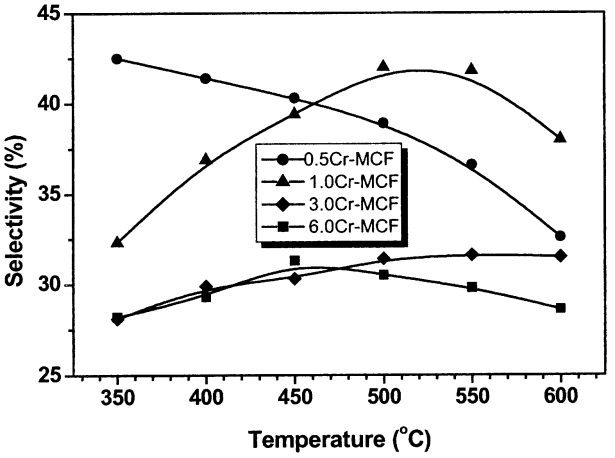

Figure 6. Dependence of selectivity to propylene on the reaction temperature during the ODH of propane over various chromium supported MCF silica catalysts (W_{cat} = 50 mg, GHSV = 15,000 ml · g^{-1}·h^{-1}).

To gain a further insight into the effect of the support structure on the ODH performance of the mesoporous silica supported chromia catalysts, the variation behavior of the selectivity to propylene with the propane conversion on the chromia dispersed on the three different siliceous supports at the same Cr loading level of 1.0 wt% is compared in figure 7. It is seen that the selectivity to propylene decreases with propane conversion in all three Cr-containing samples. By correlation with the PSD data in table 1, it was found that the Cr-containing mesoporous MCF is more active and selective than Cr–MCM or Cr–SBA catalysts loaded with comparable amount of chromium. Obviously, the superior catalytic performance of the present Cr–MCF catalyst can be understood by its favorable molecular transport properties rendered by the unique mesocellular structure with ultralarge mesopore diameter of the MCF material, which allows better diffusion of the

produced propylene to the outside of the pore during the ODH of propane, consequently preventing the subsequent deep oxidation.

Previous investigations concerning the use of transition metal oxide-based catalysts for ODH of propane have revealed that the catalysts based on supported vanadia and molybdena are highly selective and active for propane ODH, while chromium oxides dispersed on various supports are only moderately active and selective to the ODH of propane [9–17]. Recently, promising low temperature activities have been obtained over chromium-containing MCM-41 and SBA-15 materials possessing hexagonally ordered pore structures, which however can only afford maximum propylene yield of up to 5% due to the intrinsic low selectivities toward propylene formation associated with the Cr–MCM catalysts [19,27]. In the present case, the results show that the ODH of propane could proceed much more effectively over a novel mesoporous Cr-containing MCF silica catalyst system featuring a well-defined three-dimensional, continuous, ultralarge mesopore structure. The chromium supported MCF catalyst obtained by a simple impregnation of the alcoholic solution of $Cr(NO_3)_3{\cdot}9H_2O$ has demonstrated a unique catalytic behavior in ODH of propane as compared to the catalysts prepared by using conventional MCM-41 and SBA-15 as silica supports in terms of propane conversion and propylene yield. It is remarkable that a maximum propylene yield of 13.8% could be achieved over the 1.0Cr–MCF catalyst at a relatively low temperature of 550 °C.

On the other hand, it is well documented that propane conversion over Cr-based catalysts greatly depends on a number of parameters such as the oxidation state, coordination number, aggregation state and reducibility of chromium species, the acid/base properties as well as the chromium content of the catalysts, all of which have to be considered in order to account for the observed catalytic behavior for the selective oxidation of propane [17,18]. Generally, catalyst with high chromium dispersion shows better performance in the selective oxidation of propane [19,27]. The presence of isolated tetrahedral Cr species is essential for maintaining high conversion and selectivity in the ODH reaction of propane, whereas polymeric chromium species could favor undesired combustion reaction pathways, leading to the formation of carbon oxides [27]. In the present work, we have unambiguously demonstrated the unique advantage of MCFs as a new, promising support for the generation of novel Cr-containing MCF materials with favorable molecular transport properties. As a result, the ODH performance of the 3D mesocellular structured Cr–MCF catalysts is much higher than their conventional hexagonally ordered counterparts, inferring that apart from the dispersion of the active redox sites, the mass transfer properties of the catalyst also plays an important role in the gas phase selective oxidation reactions.

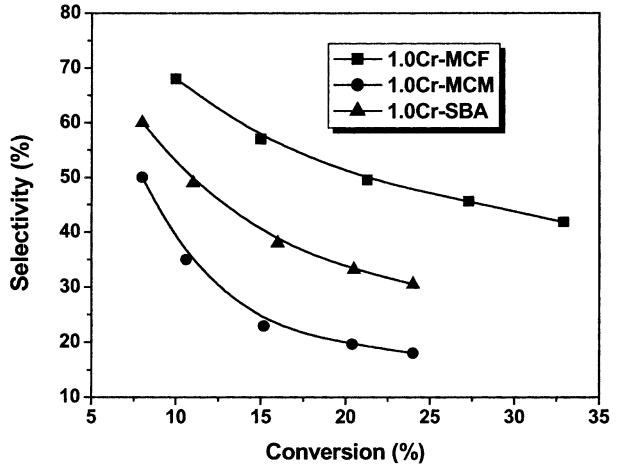

Figure 7. Variation of the selectivity to propylene with propane conversion obtained during the oxidation of propane at 550 °C on supported chromia catalysts. Catalysts: (a) 1.0Cr–MCF; (b) 1.0Cr–SBA; (c) 1.0Cr–MCM.

4. Conclusions

Mesocellular silica foams supported chromium catalysts have been prepared and characterized for ODH of propane. Mesoporous siliceous MCF materials have shown to be new promising supports for development of high performance chromium supported catalysts applicable in ODH reactions. Combined DR UV–Vis, UV Raman, and H_2-TPR results demonstrated that isolated chromium oxide species are well dispersed on the surface of mesoporous MCF silica. The as-prepared chromium-containing MCF catalysts show a high reactivity as well as moderate selectivity in the ODH of propane even at temperature as low as 350 °C. Our results show that the highest catalytic performance is attained with a 1.0 wt% chromium catalyst, with a maximum propylene yield of ~13.8%. The high catalytic activity of Cr–MCF catalysts for the ODH of propane has been attributed to the unique mesocellular pore-solid architecture with ultralarge pore diameters as well as relatively low surface acidity in the MCF catalysts.

Acknowledgements

The financial supports from National Science Foundation of China (Grant No. 20473021, 20421303, 20203003), the Major State Basic Research Development Program (Grant No. 2003CB615807) and the Committee of Shanghai Science and Technology (Grant No. 02QA14006) are gratefully acknowledged.

References

[1] B.K. Warren and S.T. Oyama, *Heterogeneous Hydrocarbon Oxidation*, 638 Vol. (American Chemical Society, Washington, DC, 1996).
[2] H.H. Kung, Adv. Catal. 40 (1994) 1.
[3] B.M. Weckhuysen and R.A. Schoonheydt, Catal. Today 51 (1999) 215.
[4] M.A. Chaar, D. Petal, M.C. Kung and H.H. Kung, J. Catal. 105 (1987) 483.
[5] C. Mazzocchia, C. Aboumrad, C. Diagne, E. Tempesti, J.M. Herrmann and G. Thomas, Catal. Lett. 10 (1991) 181.
[6] M. Chaar, D. Patel, M. Kung and H.H. Kung, J. Catal. 463 (1988) 109.
[7] T. Blasco and J.M. López-Nieto, Appl. Catal. A 157 (1997) 117.
[8] J.R.H. Ross, R.H.H. Smits and K. Seshan, Catal. Today 16 (1993) 503.
[9] A. Corma, J.M. Lopez Neito and N.J. Paredes, J. Catal. 144 (1993) 425.
[10] H.H. Kung and M.C. Kung, Appl. Catal. A 157 (1997) 105.
[11] Y.M. Liu, Y.Cao, K.K. Zhu, S.R. Yan, W.L. Dai, H.Y. He and K.N. Fan, Chem. Commun. (2002) 2832.
[12] D.L. Stern and R.K. Grasselli, J. Catal. 167 (1997) 550.
[13] B. Solsona, T. Blasco, J.M. López Nieto, M.L. Peña, F. Rey and A. Vidal-Moya, J. Catal. 443 (2001) 203.
[14] Y. Takita, H. Yamashita and K. Moritaka, Chem. Lett. (1989) 1903.
[15] D.W. Flick and M.C. Huff, Appl. Catal. A: Gen. 187 (1999) 13.
[16] S.M. Al-Zahrani, N.O. Elbashir, A.E. Abasaeed and M. Abdulwahed, Ind. Eng. Chem. Res. 40 (2001) 781.
[17] Q. Zhang, Y. Wang, Y. Ohishi, T. Shihido and K. Takehira, J. Catal. 202 (2001) 308.
[18] Y. Wang, Q.H. Zhang, Y. Ohishi, T. Shishido and K. Takehira, Catal. Lett. 72 (2001) 215.
[19] X.Z. Zhang, Y.H. Yue and Z. Gao, Catal. Lett. 83 (2002) 19.
[20] P. Schmidt-Winkel, W.W. Lukens, D.Y. Zhao, P.D. Yang, B.F. Chmelka and G.D. Stucky, J. Am. Chem. Soc. 121 (1999) 254.
[21] P. Schmidt-Winkel, W.W. Lukens, P.D. Yang, D.I. Margolese, J.S. Lettow, J.Y. Ying and G.D. Stucky, Chem. Mater. 12 (2000) 686.
[22] A. Ungureanu, D.T. On, E. Dumitriu and S. Kaliaguine, Appl. Catal. A: Gen. 254 (2003) 203.
[23] D.T. On, A. Ungureanu and S. Kaliaguine, Phys. Chem. Chem. Phys. 5 (2003) 3534.
[24] Y.M. Liu, Y. Cao, N. Yi and K.N. Fan, J. Catal. 224 (2004) 417.
[25] B.M. Weckhuysen, I.E. Wachs and R.A. Schoonheydt, Chem. Rev. 96 (1996) 3327.
[26] M. Cherian, M.S. Rao, W.T. Wang, J.M. Jehng, A.M. Hirt and G. Deo, Appl. Catal. A: Gen. 233 (2002) 21.
[27] J. Santamaría-González, J. Mérida-Robles, M. Alćantara-Rodríguez, P. Maireles-Torres, E. Rodríguez-Castellón and A. Jiménez-López, Catal. Lett. 64 (2000) 209.
[28] K. Takehira, Y. Ohishi, T. Shishido, T. Kawabata, K. Takaki, Q.H. Zhang and Y. Wang, J. Catal. 224 (2004) 404.
[29] H. Kosslick, G. Lischke, G. Walther, W. Storek, A. Martin and R. Fricke, Microporous Mater. 9 (1997) 13.
[30] E.P. Parry, J. Catal. 2 (1963) 371.
[31] H. Berndt, A. Martin, A. Brückner, E. Schreier, D. Müller, H. Kosslick, G.-U. Wolf and B. Lücke, J. Catal. 191 (2000) 384.
[32] B.M. Weckhuysen and I.E. Wachs, J. Phys. Chem. 100 (1996) 14437.
[33] A. Khodakov, J. Yang, S. Su and E. Iglesia, J. Catal. 177 (1998) 343.
[34] I.E. Wachs, Catal. Today 27 (1996) 437.